Hindawi Publishing Corporation
International Journal of Photoenergy
Volume 2012, Article ID 548158, 9 pages
doi:10.1155/2012/548158

Research Article

Ta/TiO_2-and Nb/TiO_2-Mixed Oxides as Efficient Solar Photocatalysts: Preparation, Characterization, and Photocatalytic Activity

Hussein Znad, Ming H. Ang, and Moses O. Tade

Chemical Engineering Department, Curtin University, GPO Box U 1987, Perth, WA 6845, Australia

Correspondence should be addressed to Hussein Znad, h.znad@curtin.edu.au

Received 7 December 2011; Accepted 15 December 2011

Academic Editor: Jiaguo Yu

Ta/TiO_2- and Nb/TiO_2-mixed oxides photocatalysts were prepared by simple impregnation method at different TiO_2 : Nb or Ta mass ratios of 1 : 0.1, 1 : 0.5, and 1 : 1, followed by calcination at 500°C. The prepared powders have been characterized by XRD, XPS, UV-Vis spectra, and SEM. The photocatalytic activity was evaluated under natural solar light for decolorization and mineralization of azo dye Orange II solution. The results showed that Nb/TiO_2- and Ta/TiO_2-mixed oxides have higher activity than the untreated TiO_2 under natural solar light. The maximum activity was observed for Nb/TiO_2 sample (at mass ratio of 1 : 0.1), which is characterized by the smallest crystalline size (17.79 nm). Comparing with the untreated TiO_2, the solar decolorization and mineralization rates improved by about 140% and 237%, respectively, and the band gap reduced to 2.80 eV. The results suggest that the crystal lattices of TiO_2 powder are locally distorted by incorporating Nb^{5+} species into TiO_2, forming a new band energy structure, which is responsible for the absorption in the visible region. Unlike Ta/TiO_2, the Nb/TiO_2-mixed oxides can prevent the grain size growth of the treated TiO_2, which is important to achieve high solar photoactivity.

1. Introduction

Titanium dioxide (TiO_2) is nontoxic, efficient photo-catalyst, chemically stable, and relatively inexpensive. Although TiO_2 is the most popular photocatalytic material, it has not been applied widely in the field of environmental pollution control under solar light. The band gap (E_g) of TiO_2 anatase is ~3.2 eV and lies in the UV range so that only 5–8% of sunlight photons have the required energy to activate the catalyst [1, 2]. This relatively large band gap has significantly limited its application, particularly under solar and/or visible light. An effective way to improve the TiO_2 photocatalytic activity is to introduce foreign metal ions as dopants into its lattice. Depending on the dopant type and concentration, the band gap of TiO_2 can be tailored to extend the photo responsiveness into the visible light region. Usually, the UV activity of undoped TiO_2 is much greater than the visible light activity of the doped material. Therefore, for solar applications, the photocatalysts should be tested under simulated solar irradiation or under real sun conditions [3].

TiO_2 doped with Tantalum (Ta) and niobium (Nb) by sol-gel method has been widely used in gas sensing film application [4–6]. Generally those metal dopants (Ta and Nb) are used in sensor applications to inhibit the TiO_2 phase transformation from anatase to rutile and to hinder grain growth during heating. Niobium oxide and, in particular, its most stable form, Nb_2O_5, is an interesting semiconductor with a band gap of about 3.9 eV (decreasing to about 3.5 eV in the amorphous state), with a high dielectric constant and high index of refraction, which has found important applications in electronics and optical applications, including thin films (antireflective coatings, solar control, etc.) [7].

Atashbar et al. [8] prepared thin films of TiO_2 doped with niobium oxide, for use in oxygen sensing applications. Thick film gas sensors made by Nb- or Ta-doped TiO_2 have also been prepared and investigated for atmospheric pollutant monitoring [5]. Vanadium and tantalum-doped titanium oxide (TiTaV) as a novel material for gas sensing has been prepared by Carotta et al. [4]. Furubayashi et al. [9] pointed out that Nb-doped anatase TiO_2 film has excellent electrical conductivity and transparency.

Table 1: Composition of prepared samples.

Sample reference	TiO_2 : Nb (mass ratio)	Nb molar %	Sample reference	TiO_2 : Ta (mass ratio)	Ta molar %
Pure TiO_2	1 : 0	0	Pure TiO_2	1 : 0	0
TNb1	1 : 0.1	2.9	TTa1	1 : 0.1	1.8
TNb2	1 : 0.5	13	TTa2	1 : 0.5	8.3
TNb3	1 : 1	23	TTa3	1 : 1	15.3

Technological interest in Nb-doped TiO_2 derives from the fact that Nb doping leads to enhanced photocatalytic activity in the destruction of organochloride pollutants such as dichlorobenzene [10]. Some investigators [11–13] reported that photocatalytic activity of Nb-doped TiO_2 was much better than that of pure TiO_2. Castro et al. [11] prepared Nb-doped TiO_2 by a simple, lowcost, and low-temperature hydrothermal technique. The Nb-doped TiO_2 was more active than undoped TiO_2 for diquat degradation under UV light irradiation. Yang et al. [14] prepared micrometer-sized Nb-doped TiO_2 porous spheres by ultrasonic spray pyrolysis method. Comparing with pure TiO_2, the prepared Nb-doped TiO_2 enhanced photocatalytic activity for the photodegradation of aqueous methylene blue solution under both visible and solar light irradiation. The enhanced photocatalytic activities of Ta codoped TiO_2 thin films under visible light have also been reported by Obata et al. [15].

However, to our knowledge, the photocatalytic activity of Nb/TiO_2- and Ta/TiO_2-mixed oxides for wastewater treatment under natural solar light, has not yet been reported. Furthermore, modifying the commercial TiO_2 (Degussa P25), which is relatively cheap and commercially available, to improve its solar photoactivity are an interesting subject.

Very limited attempts were found recently in the literature to improve the Degussa P25 photoactivity [16, 17]; in both cases, the photocatalyst activity was tested only under UV light. For photocatalytic hydrogen production, Yu et al. successfully improved the commercial P25 TiO_2 by impregnation with copper nitrate followed by calcinations at 350°C [18], and by a simple precipitation method using Ni $(OH)_2$ clusters [19]. Zhao et al. [20] fabricated ordered titanate nanoribbon (TNR)/SnO_2 films by electrophoretic deposition (EPD) using hydrothermally prepared titanate (P25 Degussa) as a precursor. The photocatalytic activity was evaluated by decolorization of RhB aqueous solution under UV irradiation. Shang et al. [21] prepared N-doped TiO_2 powder by annealing commercial TiO_2 (P25) under an NH_3 flow at 550°C. 4-chlorophenol decomposition was used to evaluate the photocatalytic activity under the visible light irradiation. Qi et al. [22] and Yu et al. [23] used the commercial P25 to prepare Pt/TiO_2 catalysts and CdS-sensitized Pt/P25 for photocatalytic hydrogen production. Recently, Znad and Kawase [1] successfully doped the commercial TiO_2 (Degussa P25) with a nonmetal dopant (sulfur) and improved its solar photo-catalytic activity for decolourizing polluted wastewater.

In the present work, with the aim of developing more efficient and cost-effective solar photocatalyst and to investigate the metal ions (such as Nb and Ta) influence, the Ta/TiO_2- and Nb/TiO_2-mixed oxides photocatalysts have been prepared by simple impregnation method using the well-known TiO_2 (Degussa P25) as a Ti precursor and, respectively, niobium oxide (Nb_2O_5) and tantalum oxide (Ta_2O_5) as a metal oxides. Nb and Ta ions were chosen since these elements have ionic radii similar to that of Ti, so that they could replace it in a substitutional solution with negligible distortion of the lattice. Concentrations higher than the solubility limits have been chosen to study the possible segregation of a mixed oxide.

This work was mainly devoted to find out whether the metal ions (Nb and Ta) can improve the photocatalytic activity (or properties) of TiO_2 under natural solar light, beside its well-known activity in film sensing application.

2. Experimental

2.1. Preparation of Ta/TiO_2- and Nb/TiO_2-Mixed Oxides Photocatalyst. The Ta/TiO_2- and Nb/TiO_2-mixed oxides photocatalysts were prepared by a simple impregnation method. The mass ratios for the different samples are shown in Table 1. For comparison, untreated Degussa P25 TiO_2 (pure TiO_2) was used in this work. Degussa P25 is a mixture of anatase and rutile (80 : 20) with a BET surface area of about 52.4 m^2/g and average primary particle size of about 20 nm.

In a typical preparation (described for sample TTa2 = 1 : 0.5 as representative of the series), Tantalum oxide Ta_2O_5 (0.5 g, 1.13 mmol) was suspended in 30 mL ethanol under stirring. 1 g (12.52 mmol) of Degussa P25 TiO_2 powder was suspended in 30 mL ethanol and the suspension then sonicated for 1 h at room temperature. The two suspensions of TiO_2 and Nb_2O_5 or Ta_2O_5 were mixed under vigorous stirring for 4 hours at room temperature and then dried under vacuum to obtain a powder which was further dried in oven for 8 h at 80°C. The obtained powder, was ground and then calcinated at 500°C for 3 h in the presence of air with a ramp rate of 2°C/min.

2.2. Characterization. The crystalline structure of the prepared Ta/TiO_2- and Nb/TiO_2-mixed oxides photocatalysts was characterized by X-ray powder diffraction (XRD) analysis (RINT Ultima III, Rigaku co., Japan) using Cu Ka radiation at a scan rate of 4 degree/min. The acceleration voltage and the applied current were 40 kV and 40 mA, respectively. The mean size of crystallite (D, nm) was calculated from full-width at half maxima (FWHM) of corresponding X-ray diffraction peaks using Scherrer's formula $D = 0.89\lambda/\beta \cos\phi$, where λ is the wavelength of the X-ray radiation (λ = 1.54056 nm Cu Ka), β is the full-width at half maximum (rad), and ϕ is the reflect angle. The content of anatase

w_A (%) was determined according to the following equation [24]: $w_A\ (\%) = \{I_A/(I_A + 1.265I_R)\} \times 100$, where I_R and I_A are the intensities of the diffraction peaks of rutile (110) and anatase (101), respectively, obtained from XRD patterns. X-ray photoelectron spectra (XPS) of the powders were measured using Shimadzu ESCA 750 photoelectron spectrometer with an MgKα 1253.6 ev; the shift of binding energy due to relative surface charging was corrected using the C1s level at 285 eV as an internal standard. The diffuse reflectance UV-Vis spectra were measured with an Ocean Optics high-resolution HR4000 USB spectrometer (HR4000 Ocean Optics Inc.) with an extended wavelength range from 190 to 1100 nm. The microstructures of the samples were observed by a scanning electron microscope, SEM (JSM-5310LV, Jeol Co., Japan).

2.3. Photocatalytic Activity Measurement. Solar photocatalytic decolorization and mineralization of Orange II dye was carried out in 300 mL Pyrex glass beaker. All the reactions were carried out according to the following procedure: 0.4 g of photocatalyst (modified or unmodified TiO_2) was added to 250 mL of aqueous dye (Orange II) solution (20 mg/L). The dyes solution was mixed with a magnetic stirrer during the course of the experiment. At the beginning, the solution mixture was stirred for 30 min in the dark to ensure establishment of the dye's equilibrium adsorption/desorption. Then sun light was allowed to irradiate the reaction mixture, and at regular time intervals, samples were taken from the suspension and the change of Orange-II concentration was measured using UV-Vis spectrophotometer (TU-1900 UV spectrometer) at fixed wavelength of 486 nm. For this purpose, the photocatalyst was immediately removed from the sample by filtration, using a 0.4 μm syringe filter. Solar experiments were carried out from 10:00 AM to 5:00 PM during May in Saitama, Japan. During the solar experiments, the UV and the visible ranges (illuminance) of the solar light intensity were measured by the UV radiometer (UVR-2, TOPCON, with UD-36 (310–400 nm/average 365 nm) detector, Tokyo, Japan) and illuminance meter (T-10, Konica Minolta), respectively. The accumulated solar energy was calculated by [25]

$$Q_n = Q_{n-1} + \Delta t I\left(\frac{A}{V}\right), \quad \Delta t = t_n - t_{n-1}. \tag{1}$$

Q_n accumulated solar energy per unit of slurry volume (KJL^{-1}), Δt is the time difference between radiation measurements (h), I is the solar light intensity per unit of irradiation surface area measured during time interval Δt (Wm^{-2}), A is the irradiated surface area of the photoreactor (m^2), and V is the photoreactor volume (m^3).

3. Results and Discussion

3.1. Characterization of the Prepared Photocatalysts. Figures 1(a) and 1(b) show the XRD patterns of Ta/TiO_2- and Nb/TiO_2-mixed oxides photocatalysts beside the unmodified TiO_2 samples. The anatase (101) peak was used to determine the grain size by Scherer's formula. It is evident that the Nb and Ta contents significantly influenced the particle size (FWHM) and crystallinity (anatase and rutile phases) of the modified samples. It was observed that the XRD patterns of TTa1 and TNb1 samples showed no signals originating the presence of Ta_2O_5 and Nb_2O_5 metal oxides, respectively. Actually at these low concentrations (2.9 mol% Ta and 1.8 mol% Nb), Ta and Nb ions are randomly dispersed in the crystallographic sites of anatase structure. Furthermore, the absence of metal peaks could come from their ultra fine dispersion on TiO_2 particles as very small clusters or due to very low metal content.

Figure 1(a) shows the X-ray diffraction patterns for the Ta/TiO_2-mixed oxides samples, at high concentrations of 8.3% Ta and 15.3% Ta (TTa2 and TTa3 samples), the results clearly show the presence of peaks corresponding to orthorhombic Ta_2O_5 (JCPDS 79–1375) [26]. The intensities of those peaks significantly increased with increasing the Ta_2O_5 concentration mainly due to segregation. Furthermore, increasing the Ta_2O_5 concentration could not prevent the grain growth, the average crystalline size of unmodified TiO_2 (TTa0) increased from 19.50 nm to 21.80 nm for TTa3 (see SEM results). In contrary the results of the grain size analysis of Nb/TiO_2-mixed oxide photocatalyst (Figure 1(b)) showed that the grain growth of the unmodified TiO_2 (TNb0) have been retarded due to the addition of niobium ion. The crystalline size of TNb1 and TNb3 was 17.79 nm and 18 nm, respectively.

Moreover, increasing the Nb_2O_5 concentration has stabilized the anatase phase, the anatsae content for TNb1, TNb2, and TNb3 samples was about 86%. Our results are consistent with the results of Arbiol et al. [27] who studied the effect of Nb doping in samples synthesized by induced laser pyrolysis. They found that the presence of Nb substitutional ions in the anatase structure hindered the particles growth and transformation from anatase to rutile in TiO_2 nanoparticles.

The above trend of XRD results is in agreement with the SEM analysis that indicates a decrease of the TNb particle size, as the Nb ion prevents the grain growth [28]. SEM analysis was used to attain morphological structure of the investigated photocatalysts.

The SEM images of the Ta/TiO_2- and Nb/TiO_2-mixed oxides samples besides the unmodified TiO_2 sample (TNb1, TTa1, and unmodified TiO_2) are shown in Figure 2. The SEM image of unmodified TiO_2 (Figure 2(a)) reveals that the powder consists of large micron-scale spherical agglomerates, which consist of tightly packed nanoparticles. For TTa1 sample (Figure 2(b)), some large particles obviously appear. It can be deduced that the appearing large particles may be due to the agglomeration of nanoparticles during the heat treatment. However, TNb1 sample (Figure 2(c)) seems to be relatively homogenous and to contain no large particles. The powder that possesses a sponge-like structure was found to be fine and slightly agglomerate. This structure is beneficial to enhancing the adsorption of reactants [29].

XPS spectra of the unmodified TiO_2-, Nb/TiO_2– and Ta/TiO_2-mixed oxides powders are shown in Figure 3(a) for Ti 2p, Figure 3(b) for Nb 3d, and Figure 3(c) for Ta 4f. Figure 3(a) shows that the peak position of Ti $2p_{3/2}$ corresponds to that of the Ti^{4+} oxidation state [1]. It appears that

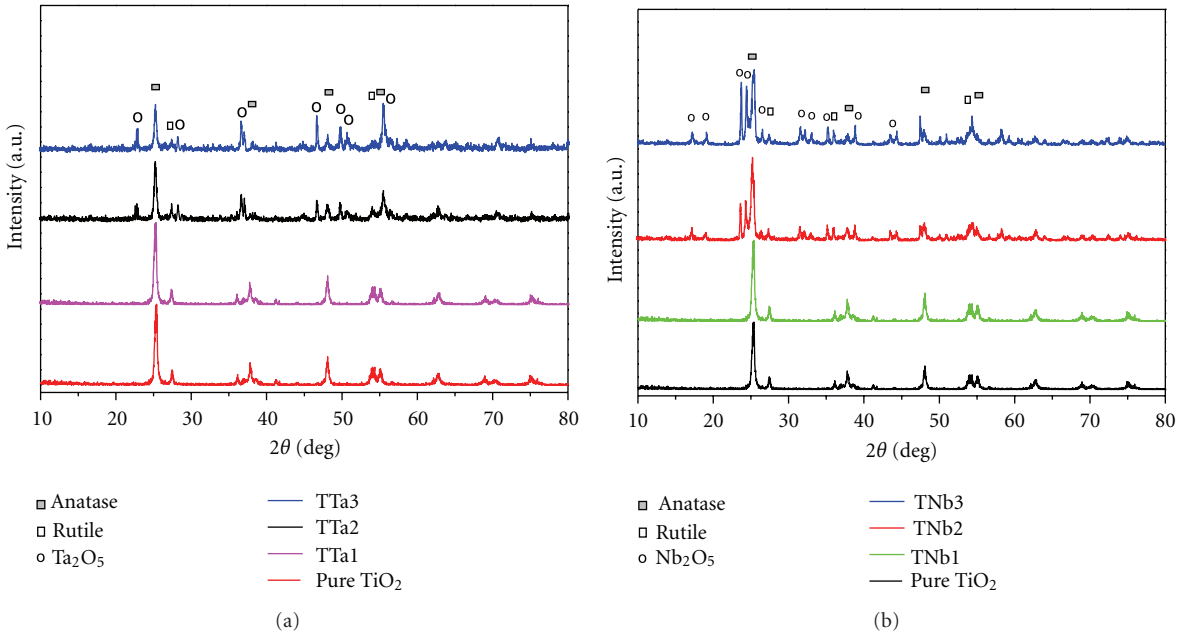

Figure 1: (a) XRD results for untreated (pure TiO_2) and Ta/TiO_2-mixed oxides at different TiO_2 : Ta ratios and 500°C calcination temperature for 3 hours. (b) XRD results for untreated (pure TiO_2) and Nb/TiO_2-mixed oxides at different TiO_2 : Nb ratios and 500°C calcination temperature for 3 hours.

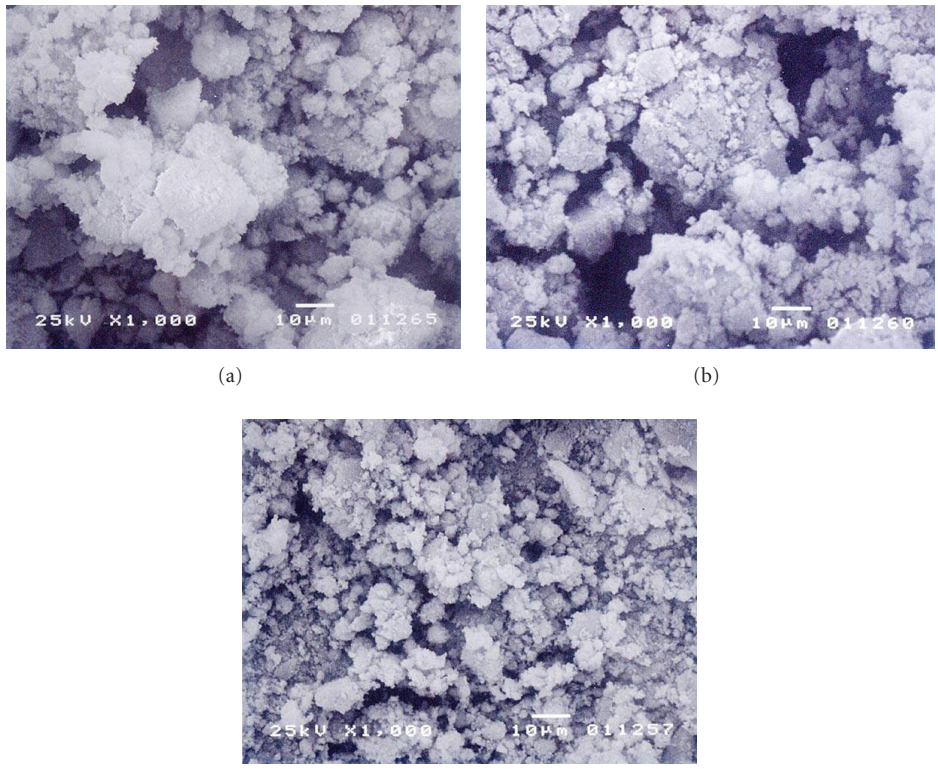

Figure 2: SEM photographs showing the untreated TiO_2 (Degussa P25) (a) and treated samples after calcinations at 500°C for 4 hours (b) Ta/TiO_2-mixed oxides (TTa1), (c) Nb/TiO_2-mixed oxides (TNb1).

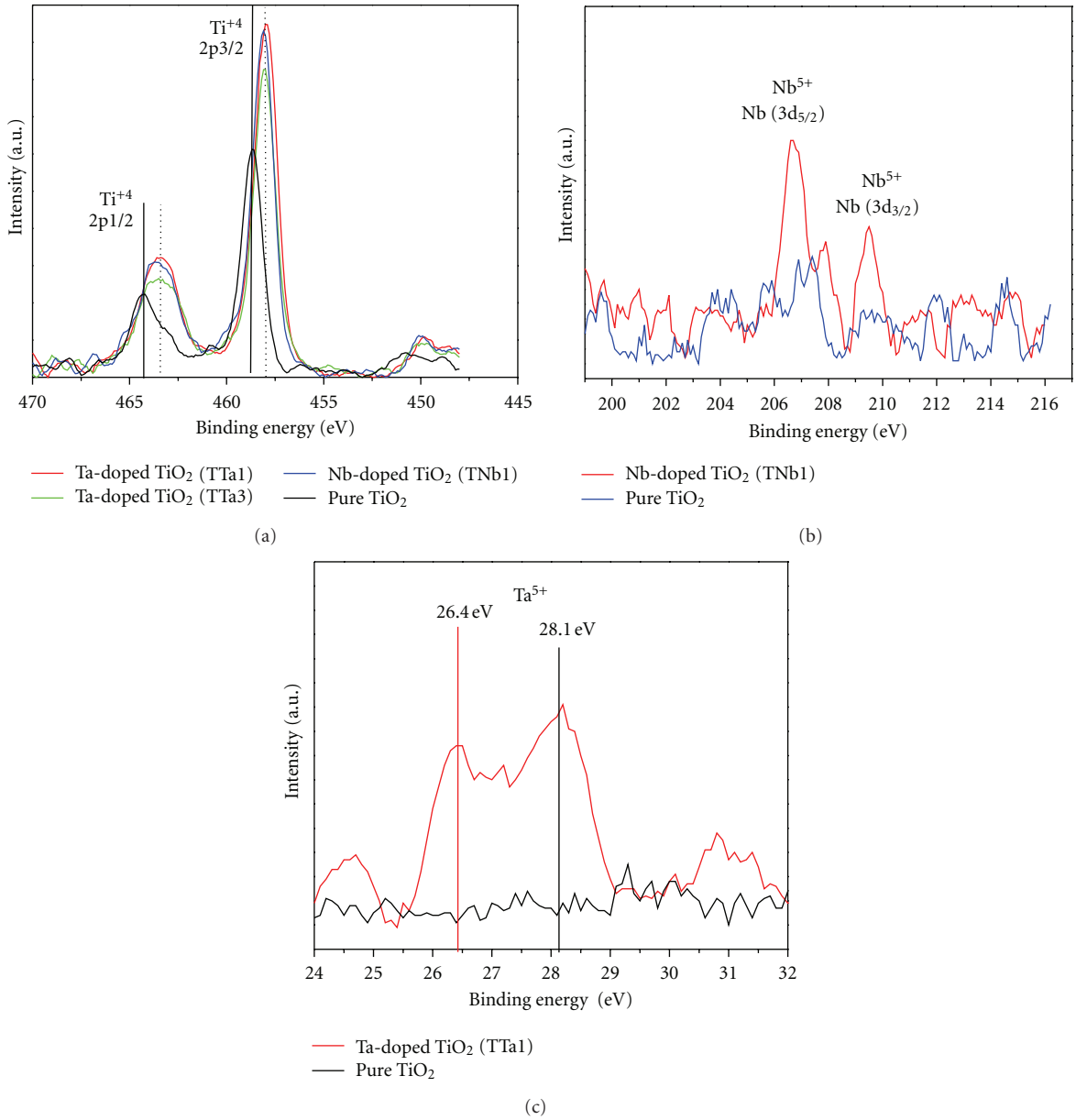

Figure 3: (a) XPS profiles of Ti2p spectra for the untreated TiO_2 (Degussa P25) and treated TiO_2 photocatalyst after calcination at 500°C for 3 hours in air. (b) Typical Nb 3d spectrum for Nb/TiO_2 mixed oxides. (c) Typical Ta 4f spectrum for Ta/TiO_2 mixed oxides.

the TiO_2 phase has been changed due to Nb and Ta species, since the full width at half-maximum (FWHM) for Ti $2p_{3/2}$ for the treated and untreated TiO_2 samples is not the same. This is in contrast to Atashbar et al. [8] who found no change in TiO_2 phase due to Nb species as the FWHM for both the Nb-treated and untreated TiO_2 was the same, which could be attributed to the low amount of Nb used in their work (1% wt). Concerning the Nb 3d spectra for Nb/TiO_2-mixed oxide (TNb1) shown in Figure 3(b), two peaks are observed at 206.7 and 209.8 eV, the peaks represent the $3d_{5/2}$ and $3d_{3/2}$ components, respectively. The center of the Nb $3d_{3/2}$ peak corresponds to that of Nb^{5+} oxidation state [8, 30]. Nb^{5+} species, substituting for Ti^{4+} in the crystalline lattice, could be a reason for anatase stabilization. Figure 3(c) shows the XPS results for Ta 4f spectra for Ta/TiO_2-mixed oxide (TTa1). The peaks at 26.4 eV and 28.1 eV were assigned to Ta^{5+} [15]. No impurities, such as Ta_2O_5, were observed for the sample at 1.8 mol% Ta (TTa1), indicating that the Ta ion was substituted at Ti sites. Therefore, it can be concluded that the oxidation state of both tantalum and niobium ions in titania (anatase) is +5. Several authors [31, 32] have illustrated that both Nb^{5+} and Ta^{5+} ions substitute for Ti^{4+} ions in normal lattice sites. In order to maintain the equilibrium of charges, the extrapositive charge due to Nb^{5+} or Ta^{5+} may be compensated by the creation of an equivalent amount of Ti^{3+} ions [33] or by the presence of vacancies in the cation sites [34]. Oxygen vacancies facilitate visible light absorption by generating discrete states about 0.75 eV and 1.18 eV below

Table 2: Characterization of the prepared samples.

Sample	Crystalline size, D (nm)	Anatase content (%)	Band gap (eV)	Decolorization rate, K_{ap} (min^{-1})
Pure TiO_2	19.50	80.02	3.10	0.0152
Nb/TiO_2 (TNb1)	**17.79**	**86.03**	**2.80**	**0.0364**
Nb/TiO_2 (TNb3)	18.00	85.70	2.93	0.0216
Ta/TiO_2 (TTa1)	20.74	75.50	3.01	0.0212
Ta/TiO_2 (TTa3)	21.80	82.01	2.98	0.0192

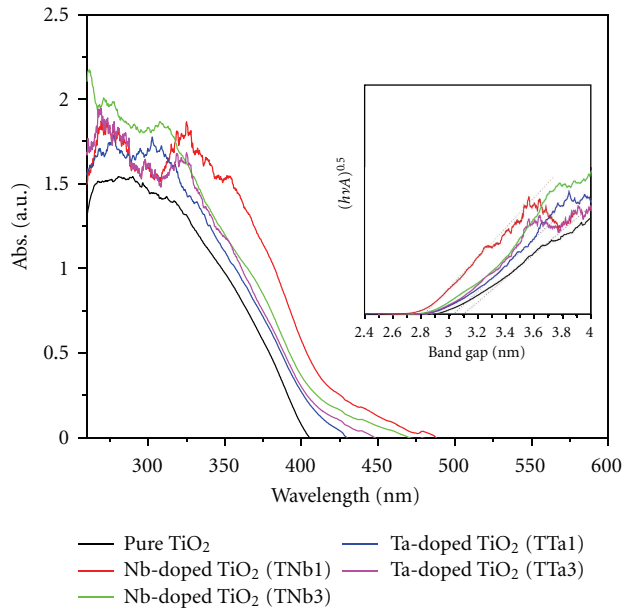

Figure 4: UV-vis diffuse reflectance spectra of the Ta/TiO_2, Nb/TiO_2, and untreated TiO_2 at different ratios. The insert Figure shows the band gap estimation.

the conduction band of titanium dioxide [35]. Oxygen vacancies are active electron traps. Since the oxygen defect states lie close to the conduction band of titania, the electrons captured by oxygen defects can be promoted to the surface by visible light absorption.

Figure 4 shows the UV-Vis absorbance spectra of the untreated TiO_2 (pure TiO_2), Ta/TiO_2-mixed oxides (TTa1 and TTa3), and Nb/Ti-mixed oxides (TNb1 and TNb3). Noticeable shifts of the optical absorption shoulders toward the visible light regions of the solar spectrum were observed for all modified photocatalysts. Notably, this shift towards the longer wavelength originates from the band gap narrowing of TiO_2 by Ta and Nb ions; this feature was more evident for (TNb1). The results clearly indicate that visible light absorption of the TiO_2 (P25 Degussa) is enhanced by introducing the Ta and Nb ions.

Estimations of the bandgap energies were obtained from the diffuse reflectance spectra of the prepared powders. The relationship between the absorption coefficient (α) and incident photon energy ($h\nu$) can be written as $\alpha = B_d(h\nu - E_g)^{0.5}/\lambda$, where B_d is the absorption constant for direct transition [36]. A plot of $(Ah\nu)^{0.5}$ versus $h\nu$ from the spectral data is shown in the insert to Figure 4. Extrapolating the linear part of the curve for the photocatalysts gives the band gap values. The linear part of the curve for the untreated TiO_2 gives a band gap value of 3.10 eV, which is very close to the commercial Degussa TiO_2 (3–3.2 eV) [37, 38]. The estimated band gap energies of the samples from Figure 4 are summarized in Table 2. The maximum band gap reduction was 0.30 eV for TNb1. It has been acknowledged that solar wavelength shows maximum irradiance at the wavelength region of 450–480 nm [39]. Since TNb1 band gap corresponds to this region, it can absorb relatively higher photon flux compared to untreated TiO_2. Probably the distortion of the local lattice of TiO_2 by Nb^{5+} and Ta^{+5} is responsible for the absorption in the visible region and to the shift of the onset of their absorption edge near 400 nm. Previous results (Figure 3) clearly showed that the crystal lattices of the TiO_2 powders are locally distorted by incorporating Nb^{5+} and Ta^{+5} species into TiO_2. These would imply that the Nb and Ta ions can form a new band above the valence band and relatively narrow the band-gap of the photocatalyst, giving rise to the absorption edge in the visible light region (Figure 4). It was found that the solar photocatalytic activity for TNb1 is better than TNb3 (Table 2). Too much of new-generated band-gap structures due to higher Nb or Ta ions concentration could act as recombination centers for electron-hole pairs and consequently reduce the photoactivity of the catalyst.

3.2. Solar Photocatalyst Activity. To evaluate the photocatalytic activity of the prepared photocatalysts (TTa1, TTa3, TNb1, and TNb3), under natural solar light irradiation, tests were carried out to decolorize and mineralize Orange II dye in an aqueous suspension at an initial Orange II concentration of 20 mg/L. Figure 5 demonstrates the solar photodecolorization and mineralization observed for Orange II in the presence of treated and untreated TiO_2 powders. It worth mentioned here that in the dark experiments there is not a definite correlation between the adsorption properties and the activity of the samples, that is, the sponge-like structure sample (TNb1) does not mean the higher the decomposition rate of Orange II dye in the dark. Xie et al. [29] got the same conclusion when comparing the photocatalytic and adsorption properties of their prepared samples.

During the course of the solar experiments, the total accumulated UV light (350–400 nm) and the total accumulated visible light (400–750 nm) were 0.457 KJ/L and 51.94 KJ/L, respectively.

A plot of $\ln(C/C_0)$ versus t represents approximate linear straight lines, showing the case of the first-order reaction.

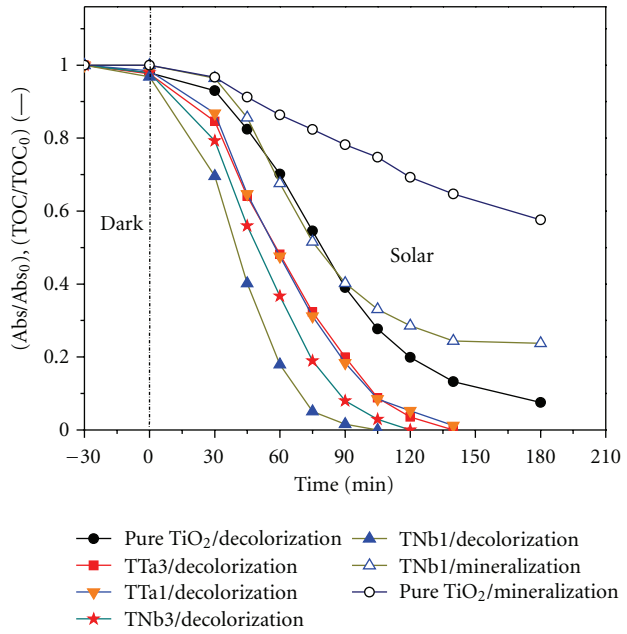

FIGURE 5: Solar photocatalytic decolorization of Orange II applying treated and untreated TiO_2. (Orange II conc. = 10 mg/L, catalyst conc. = 1.8 g/L).

The slope of the line equals the apparent first-order rate constant (K_{ap}), the estimated K_{ap} values are summarized in Table 2.

The activity of the samples was found to be dependent on the metal ions (Nb or Ta) and its amount (1 : 0.1 or 1 : 1 mass ratios). Compared with the untreated TiO_2, both Ta/Ti- and Nb/TiO_2-mixed oxides photocatalysts exhibit better photocatalytic activity, and obviously Nb/TiO_2 sample can more readily photodegrade and mineralized Orange II dye than Ta/TiO_2 sample (Table 2). The untreated-TiO_2 photocatalytic activity under solar light increased about 140% by treating with Nb at mass ratio of 1 : 0.1 (TNb1); however, it was only about 40% by treating with Ta at mass ratio of 1 : 0.1 (TTa1). Mineralization of the Orange II dye also has been tested under natural solar light (Figure 5). The TNb1 sample significantly enhanced the mineralization rate of Orange II dye (by about 237%). The stability of the catalysts has been tested by using the photocatalysts repeatedly three times (results are not shown). No visible change of the photoactivity has been observed throughout these three runs. One may raise the doubt of whether it is the photocatalyst that plays the key role in decomposing Orange II dye because the dye can absorb visible light itself. If the decomposition of Orange II dye is due to the light absorbance itself, then the efficiency of the decomposition using a different photocatalysts may not vary so much as shown in Figure 5. Orange II dye was not a subject of photolysis, and any change in Orange II dye concentration can be attributed only to the heterogeneous photocatalysis [40].

It seems that Nb ions introduce some shallow donor levels below the conduction band edge, which can act as electron traps to retard electron-hole recombination as indicated by band gap reduction in Figure 4. Therefore, the lifetime of photogenerated electrons and holes can be increased, which is beneficial to enhancing the photocatalytic efficiency [14]. It was found that the solar photocatalytic activity for TNb1 is better than TNb3 (Table 2). Higher Nb or Ta ions concentration could act as recombination centers for electron-hole pairs and consequently reduce the photoactivity of the catalyst. The excess loading of metal particles may cover active sites on the TiO_2 surface thereby reducing photodegradation efficiency [40]. Yu et al. [41] and Zhou et al. [42] pointed out that the photocatalytic activity of the metal dopants (Fe^{3+} ions) is strongly dependent on the dopant concentration since the metal ion (Fe^{3+}) can serve not only as a mediator of interfacial charge transfer but also as a recombination center. Also the morphology and surface structure (Figure 2) as well as the electronic structure of TiO_2 product modified by Nb and Ta ions should play important roles in enhancing photoactivity [43]. An efficient way to enhance the performance of the photocatalyst is to create the hierarchically porous structures in photocatalytic materials [44]. The solar photoactivities of Nb/TiO_2 mixed oxide powder (TNb1) are predominantly attributed to an improvement in anatase crystallinity, sponge-like surface structure, low band gap, and low particle size.

4. Conclusions

The commercially available TiO_2 photocatalyst (Degussa P25) has been treated with niobium (Nb) and tantalum (Ta) ions, employing simple impregnation method at room temperature. The prepared Nb/TiO_2- and Ta/TiO_2-mixed oxide powders showed higher activity than the untreated TiO_2 under natural solar light. The maximum activity was observed for Nb/TiO_2 sample at mass ratio of 1 : 0.1 (TNb1). Comparing with the untreated TiO_2, the solar decolorization and mineralization rates improved by 140% and 237%, respectively, and the band gap reduced to 2.80 eV and with a stabilized anatase phase (86% anatsa content). XPS results showed that the oxidation state of Ta and Nb ions in titania is +5 and leads to the substitution of Ti^{4+} by Nb^{5+} and Ta^{5+} in Nb/TiO_2 and Ta/TiO_2 samples, respectively. The results suggest that the crystal lattices of Nb/TiO_2 powder are locally distorted by incorporating Nb^{5+} species into TiO_2, forming a new band energy structure, which is responsible for the absorption in the visible region. The Nb/TiO_2 sample (TNb1) that is characterized by the smallest crystalline size (17.79 nm), not only stabilizes the anatase phase but also prevents the grain growth to some extent, which is important to achieve high solar photoactivity, while Ta/TiO_2 sample did not. Therefore, Nb/TiO_2-mixed oxide is more suitable than Ta/TiO_2 one. The metal ions (Nb or Ta) segregation become significant in the treated samples of higher than 1.8% Ta and 2.9% Nb. The solar photoactivities of Nb/TiO_2 powder are predominantly attributed to an improvement in anatase crystallinity, low band gap, and low particle size.

Acknowledgment

This research was supported by Japan Society for the Promotion of Science (JSPS) grant in aid.

References

[1] H. Znad and Y. Kawase, "Synthesis and characterization of S-doped Degussa P25 with application in decolorization of Orange II dye as a model substrate," *Journal of Molecular Catalysis A: Chemical*, vol. 314, no. 1-2, pp. 55–62, 2009.

[2] C. Adán, A. Bahamonde, A. Martínez-Arias, M. Fernández-García, L. A. Pérez-Estrada, and S. Malato, "Solar light assisted photodegradation of ethidium bromide over titania-based catalysts," *Catalysis Today*, vol. 129, no. 1-2, pp. 79–85, 2007.

[3] B. J. Anthony, P. A. Fernandez-Ibañez, P. S. M. Dunlop, D. M. A. Alrousan, and J. W. J. Hamilton, "Photocatalytic enhancement for solar disinfection of water: a review," *International Journal of Photoenergy*, vol. 2011, Article ID 798051, 2011.

[4] M. C. Carotta, V. Guidi, C. Malagù et al., "Vanadium and tantalum-doped titanium oxide (TiTaV): a novel material for gas sensing," *Sensors and Actuators, B*, vol. 108, no. 1-2, pp. 89–96, 2005.

[5] E. Traversa, M. L. Vona, S. Licoccia et al., "Sol-gel processed TiO_2-based nano-sized powders for use in thick-film gas sensors for atmospheric pollutant monitoring," *Journal of Sol-Gel Science and Technology*, vol. 22, no. 1-2, pp. 167–179, 2001.

[6] E. Comini, M. Ferroni, V. Guidi et al., "Effects of Ta/Nb-doping on titania-based thin films for gas-sensing," *Sensors and Actuators, B*, vol. 108, no. 1-2, pp. 21–28, 2005.

[7] A. Mattsson, M. Leideborg, K. Larsson, G. Westing, and L. Österlund, "Adsorption and solar light decomposition of acetone on anatase TiO_2 and niobium doped TiO_2 thin films," *Journal of Physical Chemistry B*, vol. 110, no. 3, pp. 1210–1220, 2006.

[8] M. Z. Atashbar, H. T. Sun, B. Gong, W. Wlodarski, and R. Lamb, "XPS study of Nb-doped oxygen sensing TiO_2 thin films prepared by sol-gel method," *Thin Solid Films*, vol. 326, no. 1-2, pp. 238–244, 1998.

[9] Y. Furubayashi, T. Hitosugi, Y. Yamamoto et al., "A transparent metal: Nb-doped anatase TiO_2," *Applied Physics Letters*, vol. 86, no. 25, Article ID 252101, 3 pages, 2005.

[10] H. Cui, K. Dwight, S. Soled, and A. Wold, "Surface acidity and photocatalytic activity of Nb_2O_5/TiO_2 photocatalysts," *Journal of Solid State Chemistry*, vol. 115, no. 1, pp. 187–191, 1995.

[11] A. L. Castro, M. R. Nunes, M. D. Carvalho et al., "Doped titanium dioxide nanocrystalline powders with high photocatalytic activity," *Journal of Solid State Chemistry*, vol. 182, no. 7, pp. 1838–1845, 2009.

[12] H. C. Yao, M. C. Chiu, D. C. Tsai, and C. J. Huang, "Effect of annealing on the Nb-doped TiO_2 films prepared by DC/RF cosputtering," *Journal of the Electrochemical Society*, vol. 155, no. 9, pp. G173–G179, 2008.

[13] A. Kubacka, M. F. García, and G. Colón, "Nanostructured Ti-M mixed-metal oxides: toward a visible light-driven photocatalyst," *Journal of Catalysis*, vol. 254, no. 2, pp. 272–284, 2008.

[14] J. Yang, X. Zhang, C. Wang et al., "Solar photocatalytic activities of porous Nb-doped TiO_2 microspheres prepared by ultrasonic spray pyrolysis," *Solid State Sciences*, vol. 14, no. 1, pp. 139–144, 2012.

[15] K. Obata, H. Irie, and K. Hashimoto, "Enhanced photocatalytic activities of Ta, N co-doped TiO_2 thin films under visible light," *Chemical Physics*, vol. 339, no. 1–3, pp. 124–132, 2007.

[16] M. Janus and A. W. Morawski, "New method of improving photocatalytic activity of commercial Degussa P25 for azo dyes decomposition," *Applied Catalysis B: Environmental*, vol. 75, no. 1-2, pp. 118–123, 2007.

[17] N. Bowering, D. Croston, P. G. Harrison, and G. S. Walker, "Silver modified degussa P25 for the photocatalytic removal of nitric oxide," *International Journal of Photoenergy*, vol. 2007, Article ID 90752, 8 pages, 2007.

[18] J. Yu, Y. Hai, and M. Jaroniec, "Photocatalytic hydrogen production over CuO-modified titania," *Journal of Colloid and Interface Science*, vol. 357, no. 1, pp. 223–228, 2011.

[19] J. Yu, Y. Hai, and B. Cheng, "Enhanced photocatalytic H_2-production activity of TiO_2 by $Ni(OH)_2$ cluster modification," *Journal of Physical Chemistry C*, vol. 115, no. 11, pp. 4953–4958, 2011.

[20] L. Zhao, J. Ran, Z. Shu, G. Dai, P. Zhai, and S. Wang, "Effects of calcination temperatures on photocatalytic activity of ordered titanate nanoribbon/SnO_2 films fabricated during an EPD process," *International Journal of Photoenergy*, vol. 2012, Article ID 472958, 2012.

[21] G. Shang, H. Fu, S. Yang, and T. Xu, "Mechanistic study of visible-light-induced photodegradation of 4-chlorophenol by TiO_{2-x} N_x with low nitrogen concentration," *International Journal of Photoenergy*, vol. 2012, Article ID 759306, 2012.

[22] L. Qi, J. Yu, and M. Jaroniec, "Preparation and enhanced visible-light photocatalytic H_2 production activity of CdS-sensitized Pt/TiO_2 nanosheets with exposed (001) facets," *Physical Chemistry Chemical Physics*, vol. 13, no. 19, pp. 8915–8923, 2011.

[23] J. Yu, L. Qi, and M. Jaroniec, "Hydrogen production by photocatalytic water splitting over Pt/TiO_2 nanosheets with exposed (001) facets," *Journal of Physical Chemistry C*, vol. 114, no. 30, pp. 13118–13125, 2010.

[24] T. Ohno, M. Akiyoshi, T. Umebayashi, K. Asai, T. Mitsui, and M. Matsumura, "Preparation of S-doped TiO_2 photocatalysts and their photocatalytic activities under visible light," *Applied Catalysis A: General*, vol. 265, no. 1, pp. 115–121, 2004.

[25] M. Tokumura, H. T. Znad, and Y. Kawase, "Decolorization of dark brown colored coffee effluent by solar photo-Fenton reaction: effect of solar light dose on decolorization kinetics," *Water Research*, vol. 42, no. 18, pp. 4665–4673, 2008.

[26] K. V. Baiju, P. Shajesh, W. Wunderlich, P. Mukundan, S. R. Kumar, and K. G. K. Warrier, "Effect of tantalum addition on anatase phase stability and photoactivity of aqueous sol-gel derived mesoporous titania," *Journal of Molecular Catalysis A: Chemical*, vol. 276, no. 1-2, pp. 41–46, 2007.

[27] J. Arbiol, J. Cerdà, G. Dezanneau et al., "Effects of Nb doping on the TiO_2 anatase-to-rutile phase transition," *Journal of Applied Physics*, vol. 92, no. 2, p. 853, 2002.

[28] M. D. Koninck, P. Manseau, and B. Marsan, "Preparation and characterization of Nb-doped TiO_2 nanoparticles used as a conductive support for bifunctional $CuCo_2O_4$ electrocatalyst," *Journal of Electroanalytical Chemistry*, vol. 611, no. 1-2, pp. 67–79, 2007.

[29] Y. Xie, Y. Li, and X. Zhao, "Low-temperature preparation and visible-light-induced catalytic activity of anatase F-N-codoped TiO_2," *Journal of Molecular Catalysis A: Chemical*, vol. 277, no. 1-2, pp. 119–126, 2007.

[30] J. F. Moulder, W. F. Stickle, P. E. Sool, and K. D. Bomben, *Handbook of X-Ray Photoelectron Spectroscopy*, Perkin-Elmer Corporation, Eden Prairie, Minn, USA, 1999.

[31] A. H. Meitzler, "Structural transformations occasioned by crystallographic shear in PLZT and TiO_2 ceramics," *Ferroelectrics*, vol. 11, no. 3-4, pp. 503–510, 1975.

[32] M. Nazrullah and H. U. Anderson, "Compensation modes in counter doped Rutile," *Journal of Solid State Chemistry*, vol. 90, pp. 373–376, 1991.

[33] M. Valigi, D. Cordischi, G. Minelli, P. Natale, and P. Porta, "A structural, thermogravimetric, magnetic, electron spin resonance, and optical reflectance study of the NbO_xTiO_2

system," *Journal of Solid State Chemistry*, vol. 77, no. 2, pp. 255–263, 1988.

[34] M. Sacerdoti, M. C. Dalconi, M. C. Carotta et al., "XAS investigation of tantalum and niobium in nanostructured TiO_2 anatase," *Journal of Solid State Chemistry*, vol. 177, no. 6, pp. 1781–1788, 2004.

[35] S. Y. Dhumal, T. L. Daulton, J. Jiang, B. Khomami, and P. Biswas, "Synthesis of visible light-active nanostructured TiO_x ($x < 2$) photocatalysts in a flame aerosol reactor," *Applied Catalysis B: Environmental*, vol. 86, no. 3-4, pp. 145–151, 2009.

[36] X. H. Wang, J. G. Li, H. Kamiyama et al., "Pyrogenic iron(III)-doped TiO_2 nanopowders synthesized in RF thermal plasma: phase formation, defect structure, band gap, and magnetic properties," *Journal of the American Chemical Society*, vol. 127, no. 31, pp. 10982–10990, 2005.

[37] J. Zhao and X. Yang, "Photocatalytic oxidation for indoor air purification: a literature review," *Building and Environment*, vol. 38, no. 5, pp. 645–654, 2003.

[38] S. Perathoner, R. Passalacqua, G. Centi, D. S. Su, and G. Weinberg, "Photoactive titania nanostructured thin films: synthesis and characteristics of ordered helical nanocoil array," *Catalysis Today*, vol. 122, no. 1-2, pp. 3–13, 2007.

[39] K. Nagaveni, G. Sivalingam, M. S. Hegde, and G. Madras, "Solar photocatalytic degradation of dyes: high activity of combustion synthesized nano TiO_2," *Applied Catalysis B*, vol. 48, no. 2, pp. 83–93, 2004.

[40] V. Štengl and D. Králová, "TiO_2/ZnS/CdS nanocomposite for hydrogen evolution and orange II dye degradation," *International Journal of Photoenergy*, vol. 2011, Article ID 532578, 2011.

[41] J. Yu, Q. Xiang, and M. Zhou, "Preparation, characterization and visible-light-driven photocatalytic activity of Fe-doped titania nanorods and first-principles study for electronic structures," *Applied Catalysis B: Environmental*, vol. 90, no. 3-4, pp. 595–602, 2009.

[42] M. Zhou, J. Yu, and B. Cheng, "Effects of Fe-doping on the photocatalytic activity of mesoporous TiO_2 powders prepared by an ultrasonic method," *Journal of Hazardous Materials B*, vol. 137, no. 3, pp. 1838–1847, 2006.

[43] J. Yu, S. Liu, and H. Yu, "Microstructures and photoactivity of mesoporous anatase hollow microspheres fabricated by fluoride-mediated self-transformation," *Journal of Catalysis*, vol. 249, no. 1, pp. 59–66, 2007.

[44] J. Yu and L. Qi, "Template-free fabrication of hierarchically flower-like tungsten trioxide assemblies with enhanced visible-light-driven photocatalytic activity," *Journal of Hazardous Materials*, vol. 169, no. 1–3, pp. 221–227, 2009.